Since January 2020 Elsevier has created a COVID-19 resource centre with free information in English and Mandarin on the novel coronavirus COVID-19. The COVID-19 resource centre is hosted on Elsevier Connect, the company's public news and information website.

Journal of Virological Methods 218 (2015) 27–39

Contents lists available at ScienceDirect

Journal of Virological Methods

journal homepage: www.elsevier.com/locate/jviromet

Analysis of protein expression changes of the Vero E6 cells infected with classic PEDV strain CV777 by using quantitative proteomic technique

Dongbo Sun[a,b,*], Hongyan Shi[a], Donghua Guo[b], Jianfei Chen[a], Da Shi[a], Qinghe Zhu[b], Xin Zhang[a], Li Feng[a,*]

[a] Division of Swine Infectious Diseases, National Key Laboratory of Veterinary Biotechnology, Harbin Veterinary Research Institute of the Chinese Academy of Agricultural Sciences, No. 427 Maduan Street, Nangang District, Harbin 150001, PR China
[b] College of Animal Science and Veterinary Medicine, Heilongjiang Bayi Agricultural University, No. 2 Xinyang Road, Sartu District, Daqing 163319, PR China

Article history:
Received 2 October 2014
Received in revised form 20 February 2015
Accepted 7 March 2015
Available online 14 March 2015

Keywords:
PEDV
Infection-associated proteins
Quantitative proteomics

A B S T R A C T

Recent outbreaks of porcine epidemic diarrhea virus (PEDV) have caused widespread concern. The identification of proteins associated with PEDV infection might provide insight into PEDV pathogenesis and facilitate the development of novel antiviral strategies. We analyzed the differential protein profile of PEDV-infected Vero E6 cells using mass spectrometry and an isobaric tag for relative and absolute quantification. A total of 126 proteins were identified that were differentially expressed between the PEDV-infected and mock-infected groups ($P < 0.05$, quantitative ratio ≥ 1.2), among which the expression of 58 proteins was up-regulated and that of 68 proteins was down-regulated in the PEDV-infected Vero E6 cells, involving in integrin β2/β3, cystatin-C. The Gene Ontology analysis indicated that the molecular function of the differentially expressed proteins (DEPs) was primarily related to binding and catalytic activity, and that the biological functions in which the DEPs are involved included metabolism, organismal systems, cellular processes, genetic information processing, environmental information processing, and diseases. Among the disease-related functions, certain anti-viral pathways and proteins, such as the RIG-I-like receptor, Rap1, autophagy, mitogen-activated protein kinase, PI3K-Akt and Jak-STAT signaling pathways, and integrin β2/β3 and cystatin-C proteins, represented potential factors in PEDV infection. Our findings provide valuable insight into PEDV-Vero E6 cell interactions.

1. Introduction

The porcine epidemic diarrhea virus (PEDV) is an enveloped, single-stranded positive-sense RNA virus that causes porcine epidemic diarrhea (PED), an acute and highly contagious enteric disease in pigs. PED is characterized by severe diarrhea, vomiting, dehydration, and a mortality rate of up to 90% in suckling piglets (Pensaert and Debouck, 1978). PED was first reported in Belgium and the United Kingdom in 1978, and frequent outbreaks have occurred in various Asian countries (Chen et al., 2010). Since 2007, acute PED outbreaks have continually occurred in Thailand, China, and the USA, which have resulted in substantial economic losses (Puranaveja et al., 2009; Li et al., 2012; Chen et al., 2013; Huang et al., 2013; Marthaler et al., 2013; Stevenson et al., 2013; Yang et al., 2013; Chen et al., 2014). The continued outbreaks of PED, despite control efforts, have caused widespread concern.

The PEDV belongs to the genus *Alphacoronavirus*, in the family *Coronaviridae* and order *Nidovirales* (Belouzard et al., 2012). Previous studies have investigated various control measures to protect against PEDV infection, such as vaccines, diagnostic tools, and therapeutic drugs (Sun et al., 2008; Ren et al., 2011; Sun et al., 2012; Zhu et al., 2013; Guo et al., 2013; Kim and Lee, 2013). Various aspects of PEDV infection remain unclear, for example, swine testis (ST) cells expressing porcine aminopeptidase N of PEDV receptor were not susceptible to PEDV infection. African green monkey kidney (Vero) cells are highly susceptible to PEDV infection, and are widely used for the primary isolation and cultivation of PEDV (Pan et al., 2012; Guo et al., 2014). Therefore, Vero lineages are suitable hosts for understanding the mechanisms of PEDV infection.

* Corresponding authors at: Division of Swine Infectious Diseases, National Key Laboratory of Veterinary Biotechnology, Harbin Veterinary Research Institute of the Chinese Academy of Agricultural Sciences, No. 427 Maduan Street, Nangang District, Harbin 150001, PR China. Tel.: +86 18946066048; fax: +86 451 51997164.
E-mail addresses: dongbosun@126.com (D. Sun), fl@hvri.ac.cn (L. Feng).

http://dx.doi.org/10.1016/j.jviromet.2015.03.002
0166-0934/

Proteomics techniques are effective tools for characterizing protein expression profiles, and have been used widely to investigate disease-associated proteins (Hondermarck et al., 2008; Boja et al., 2011; He et al., 2012; Sun et al., 2013). Among current proteomics methods, quantitative high-throughput proteomics approaches are useful for the analysis of infection-associated proteins of pathogens (Linde et al., 2013; Papachristou et al., 2013; Ye et al., 2013; Zeng et al., 2015). In our current study, we used a quantitative proteomics approach based on an iTRAQ tandem mass spectrometry (MS/MS) technique to identify proteins differentially expressed between PEDV-infected and mock-infected Vero E6 cells. The functions of the differentially expressed proteins (DEPs) were analyzed to determine whether they might be associated with PEDV infection. Our findings provide valuable insight into the changes in cellular processes that occur during PEDV infection.

2. Materials and methods

2.1. Virus, cells, and antibody

The CV777 strain of PEDV, kindly provided by Maurice Pensaert at Ghent University (Merelbeke, Belgium), was used in all of our experiments after being adapted to Vero E6 cells, as previously described (Hofmann and Wyler, 1988). The Vero E6 cell-adapted PEDV, the Vero E6 cells, and the monoclonal antibody against the nucleocapsid protein (Np) of PEDV were stored at the Diarrhea-Related Viruses Section, Division of Swine Infectious Diseases, National Key Laboratory of Veterinary Biotechnology, Harbin Veterinary Research Institute of the Chinese Academy of Agricultural Sciences.

2.2. Viral infection of Vero E6 cells

The Vero E6 cells were cultured in Dulbecco's modified Eagle's medium containing 10% fetal bovine serum (FBS) in 75-cm flasks at 37 °C in a 5% CO_2 atmosphere. When the cells reached 70–80% confluence, they were inoculated with the PEDV at a multiplicity of infection of 1 in presence of 5 μg/mL trypsin. At 48 h postinoculation, the cells began to exhibit cytopathic effects (CPEs) of viral infection, but no cells lysis or shedding had occurred. The cells were washed three times with cold phosphate-buffered saline (PBS, pH 7.4). A 1.5-mL aliquot of lysis buffer containing 4% SDS, 1 mM DTT, and 150 mM Tris–HCl (pH 8.0) was added to each flask, and the flasks were incubated at 37 °C for 5 min. The cell lysates were collected using a cell scraper, and boiled for 5 min. Three cell lysate replicates were prepared for the PEDV-infected (V1–V3) and mock-infected (C1–C3) Vero E6 cells, and stored at −80 °C.

2.3. Immunoblotting

Western blotting was performed to confirm PEDV infection by detecting the presence of the Np of PEDV in the Vero E6 cells. Aliquots of the cell lysates were subjected to SDS-PAGE on a 12% acrylamide gel, and the protein bands were transferred to a nitrocellulose membrane using a semi-dry transfer device (Bio-Rad, Hercules, CA, USA). The membrane was blocked using 5% (w/v) nonfat dried milk in PBS at 37 °C for 1 h, before incubation in PBS containing the anti-Np monoclonal antibody (1:2000 dilution) at 37 °C for 1 h. After washing three times with 5% Tween 20 in PBS (PBST), the membrane was incubated in PBST containing a horseradish peroxidase-conjugated goat anti-mouse IgG (1:4000 dilution) at 37 °C for 1 h. After washing three times with PBS, the membrane was incubated with enhanced chemiluminescence detection reagents (Biotopped, Beijing, China) at room temperature for 3 min, and the peroxidase-mediated luminescence was digitally captured using the Molecular Imager ChemiDoc XRS+ System (Bio-Rad) and the Image Lab software (Bio-Rad). To verify the differential expression of the selected DEPs, equivalent volumes of the cell lysate replicates from the PEDV-infected (V1–V3) and mock-infected (C1–C3) Vero E6 cells were pooled into the V and C samples, respectively, and western blotting was performed as described above, with the following exceptions: a 1:1000 dilution of the polyclonal antibodies anti-β tubulin, anti-integrin-β3, anti-cystatin-C, anti-protein S100-A2, anti-apolipoprotein E4, and anti-centrin from rabbit (Beijing Biosynthesis Biotechnology, Beijing, China) was used as the primary antibody, and a 1:5000 dilution of the HRP-conjugated goat anti-rabbit IgG (Sigma–Aldrich, St. Louis, USA) was used as the secondary antibody.

2.4. Protein digestion and iTRAQ labeling

Protein digestion of the samples was performed according to the FASP procedure described by Wiśniewski et al. (2009). An aliquot of each cell lysate containing 200 μg of protein was combined with 30 μL of STD buffer containing 4% SDS, 100 mM DTT, and 150 mM Tris–HCl (pH 8.0). The detergent, DTT, and other low-molecular-weight components were removed by dilution in UA buffer containing 8 M Urea and 150 mM Tris–HCl (pH 8.0) and repeated ultrafiltration using Microcon (30 kDa) ultrafiltration units. The reduction of cysteine residues was blocked by the addition of 100 μL of 0.05 M iodoacetamide to the UA buffer. The samples were incubated for 20 min in darkness before ultrafiltration. The Microcon filters were washed three times with 100 μL of UA buffer, followed by two washes with 100 μL DS buffer containing 50 mM triethyl ammonium bicarbonate (pH 8.5). The final protein suspensions were digested using 2 μg of trypsin (Promega, Madison, WI, USA) in 40 μL of DS buffer overnight at 37 °C, and the digested peptides were collected as the filtrate. The peptide content was quantified based on absorbance at 280 nm using an extinction coefficient of 1.1 for a 0.1 mg/mL solution. The digested peptide mixture was labeled using the 8-plex iTRAQ reagent (Life Technologies, Carlsbad, CA, USA), according to the manufacturer's instructions. Each iTRAQ reagent was dissolved in 70 μL of ethanol, and added to the digested peptide mixture. The samples were labeled as C1-113, C2-114, C3-115, V1-116, V2-117, or V3-118. The samples were multiplexed, and vacuum dried.

2.5. Peptide fractionation with strong cation exchange chromatography (SCXC)

The iTRAQ labeled peptides were fractionated by SCXC using the AKTA Purifier system (GE Healthcare, Waukesha, WI, USA). The dried peptide mixture was reconstituted, and acidified by the addition of 2 mL of buffer A containing 10 mM KH_2PO_4 in 25% acetonitrile (pH 2.7). The samples were loaded onto a 4.6 mm × 100 mm column packed with Polysulfoethyl (5 μm, 200 Å) chromatography resin (PolyLC, Columbia, Maryland, USA). The peptides were eluted at a flow rate of 1 mL/min using a gradient of 0–10% buffer B containing 500 mM KCl and 10 mM KH_2PO_4 in 25% acetonitrile (pH 2.7). The gradient elution consisted of 10–20% buffer B for 25 min, 20–45% buffer B for 5 min, and 50–100% buffer B for 5 min. The absorbance of the eluate was monitored at 214 nm, and fractions were collected at 1-min intervals. Thirty fractions were combined into ten pools, and desalted using Empore standard density SPE C18 cartridges (Sigma–Aldrich, St. Louis, MO, USA) with a bed diameter of 7 mm and a volume 3 mL. Each fraction was concentrated by centrifugation in a vacuum, and reconstituted in 40 μL of 0.1% (v/v) trifluoroacetic acid. All samples were stored at −80 °C until the MS analysis was performed.

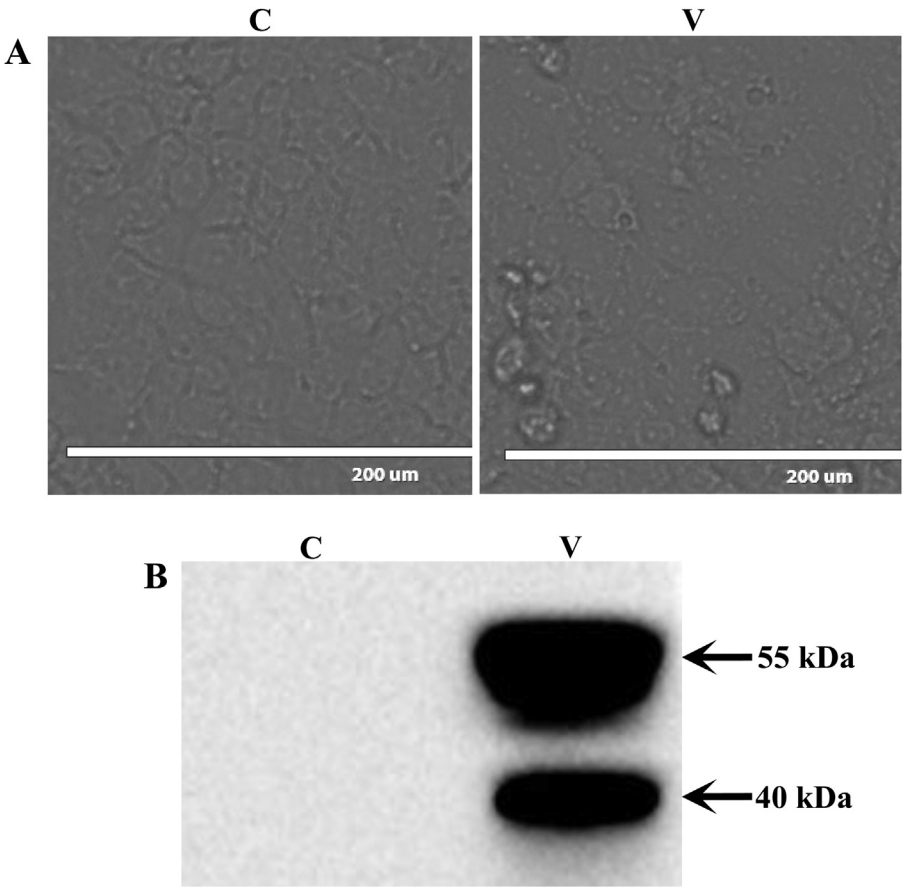

Fig. 1. Preparation and identification of PEDV-infected Vero E6 cells. (A) Photomicrographs of PEDV-infected Vero E6 cells or mock-infected Vero E6 cells: C, mock-infected group; V, PEDV-infected group. (B) Verification of PEDV propagation in Vero E6 cells by western blot: C, mock-infected group; V, PEDV-infected group.

2.6. Liquid chromatography (LC) MS/MS analysis

The LC–MS/MS experiments were performed using a Q Exactive mass spectrometer coupled to a Proxeon Biosystem Easy nanoLC (Thermo Fisher Scientific, Waltham, MA, USA). Ten microliters of each fraction was injected for nanoLC–MS/MS analysis. The peptide mixture (5 μg) was loaded onto a C18-reversed phase column (15 cm × 75 μm) packed with RP-C18 (5 μm) resin in buffer A containing 0.1% formic acid, and eluted with a linear gradient of buffer B (80% acetonitrile and 0.1% formic acid) at a flow rate of 0.25 μL/min for 140 min using the IntelliFlow technology. The eluate underwent electrospray ionization for the MS/MS analysis. The MS/MS instrument was run in the peptide recognition mode, and the spectra were acquired using a data-dependent top-10 method based on the selection of the most abundant precursor ions from the survey scan (300–1800 m/z) for HCD fragmentation. The determination of the target value was based on the predictive automatic gain control, and the dynamic exclusion duration was 60 s. Survey scans were acquired at a resolution of 70, 000 at m/z 200, and the resolution for the HCD spectra was set to 17, 500 at m/z 200. The normalized collision energy was 30 eV, and the underfill ratio, which specifies the minimum percentage of the target value likely to be reached at maximum fill time, was defined as 0.1%.

2.7. Identification and analysis of proteins

The MS/MS spectra were compared to the Uniprot *Cercopithecidae* database (107 051 sequences, downloaded November 25, 2013) and a decoy database using the MASCOT search engine, version 2.2 (Matrix Science, London, UK), embedded in the Proteome Discoverer 1.4 software (Thermo Electron, San Jose, CA). The following parameters were used for protein identification: a peptide mass tolerance of 20 ppm; an MS/MS tolerance of 0.1 Da; trypsin digestion; a missed cleavage value of 2; the fixed modifications included carbamidomethyl, iTRAQ8plex(K), and iTRAQ8plex(N-term); the variable modification was oxidation; and an FDR value ≤0.01. Protein quantification was performed using the Proteome Discoverer 1.4 software based on the centroided reporter ion peak intensity. The average quantitative value of each protein in samples C1, C2, and C3 (mock-infection group) was used as the internal reference. The value of the quantitative ratio for each protein relative to the internal reference was calculated, and averaged to obtain the quantitative ratio (V/C) of the proteins identified in the treatment groups (Unwin et al., 2010). A protein was considered to be differentially expressed between the PEDV-infected and mock-infected groups based on the following criteria: the protein had to be present in three replicates of both groups, the difference in the level of the protein between the two groups had to be statistically significant ($P < 0.05$), and the change ratio for the protein had to be ≥1.2 (Yuan et al., 2012). The expression of a protein with a $V/C > 1.0$ was considered to be up-regulated, and those with a $V/C < 1.0$ were considered to be down-regulated. The data were analyzed using a two-tailed, paired Student's t test. The statistical analysis was performed using the Excel 2007 software (Microsoft, Redmond, WA, USA). The DEPs were annotated using the Blast2GO, version 2.7.0, program (Ashburner et al., 2000; Quevillon et al., 2005; Götz et al., 2008). The DEPs were blasted against the KEGG Genes database (human). The Gene Ontology categories (GOCs) were retrieved, and mapped to pathways in the KEGG database (Kanehisa et al., 2012).

Table 1
The proteins identified from PEDV-infected and mock-infected groups.

Classification	Number of proteins (percentage)
Identified peptides	15,564
Identified proteins	3178 (100%)
Quantified proteins	3171 (99.78%)
Known proteins	1859 (58.50%)
Uncharacterized proteins	1319 (41.50%)
Annotated proteins in GO categories of biological process	2061 (64.85%)
Annotated proteins in GO categories of molecular function	2495 (78.51%)
Annotated proteins in GO categories of cellular component	1917 (60.32%)

3. Results

3.1. Identification and analysis of proteins

The Vero E6 cells inoculated with PEDV displayed distinct CPEs at 48 h postinoculation, including cell shrinkage, cell fusion, and a rounded cell morphology, but no cells lysis or shedding was observed (Fig. 1A). The immunoblotting analysis confirmed that the Vero E6 cells were PEDV-infected. The band corresponding to the Np of PEDV was detected in samples V1, V2, and V3, whereas none was detected in samples C1, C2, and C3 (Fig. 1B). The identified peptides, identified proteins, quantified proteins, known/uncharacterized proteins, and the GOC annotations are showed in Table 1. A total of 3178 proteins, including 15 564 peptides, were identified in the PEDV-infected and mock-infected groups using the iTRAQ-MS/MS approach, among which 3171 (99.78%) were quantified, 1859 (58.50%) were known proteins, and 1319 (41.50%) were uncharacterized/putative proteins. Based on the GOCs, 2061 (64.85%) of the proteins were annotated as biological process, 2495 (78.51%) were annotated as molecular function, and 1917 (60.32%) were annotated as cellular components.

The quantification and significance of the identified proteins are shown in Fig. 2. The changes in the levels of expression between the two groups were analyzed based on statistical significance. Of the 3178 proteins identified, 2496 (78.54%) were not differentially expressed ($P > 0.05$), and 675 (21.24%) were expressed at statistically different levels between the PEDV-infected and mock-infected Vero E6 cells ($P < 0.05$), including 357 proteins (11.23%) with a P-value between 0.01 and 0.05, 227 proteins (7.14%) with a P-value between 0.001 and 0.01, and 91 proteins (2.86%) with a P-value <0.001. The proteins with a P-value <0.05 were also filtered based on whether the V/C or C/V was ≥1.2. Based on these criteria, a total of 126 (3.96%) of the 3178 identified proteins were determined to have been differentially expressed between the PEDV-infected and mock-infected groups (Table 2). Among the 126 DEPs, 46.03% (58/126) were up-regulated, and 53.97% (68/126) down-regulated. The known proteins and uncharacterized/putative proteins accounted for 69.05% (87/126) and 30.95% (39/126) of the DEPs, respectively. The DEP displaying the greatest increase in expression in the PEDV-infected Vero E6 cells was isoform 2 of the ovarian cancer immunoreactive antigen domain-containing 1 protein (1:2.5), and the DEP displaying the greatest decrease in expression in the PEDV-infected Vero E6 cells was cystatin-C (1:2.2).

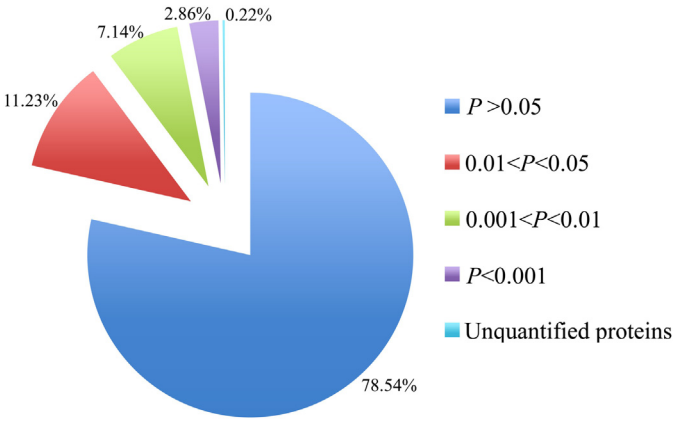

Fig. 2. The quantitation and significance of the 3178 identified proteins from PEDV-infected and mock-infected groups.

3.2. GO annotations of the DEPs

The Gene Ontology (GO) database has been widely used for describing protein function in a standardized format. According to their GOCs, the 126 DEPs were annotated as cellular component, biological process, or molecular function. The GO annotations are shown in Table 2, and distributions of the GO annotations are shown in Fig. 3. Seventy-eight DEPs were distributed among 16 groups of biological processes (Fig. 3A). The metabolic process (GO:0008152), cellular process (GO:0009987), single-organism process (GO:0044699), and biological regulation (GO:0065007) groups contained the highest proportions of the biological process DEPs. There were more up-regulated proteins in the cellular component organization group (GO:0071840) than down-regulated proteins. Seventy-four DEPs were distributed among eight cellular component groups (Fig. 3B), among which the organelle (GO:0043226) and cell (GO:0005623) groups contained the highest proportion of cellular component DEPs. There were more down-regulated DEPs in the membrane group (GO:0016020) than up-regulated DEPs, and there were more up-regulated DEPs in the macromolecular complex group (GO:0032991) than down-regulated DEPs. Ninety-seven DEPs were distributed among eight molecular function groups (Fig. 3C), among which the binding (GO:0005488) and catalytic activity (GO:0003824) groups contained the greatest proportion of molecular function DEPs.

3.3. KEGG pathway analysis of the DEPs

The kyoto encyclopedia of genes and genomes (KEGG) pathway is a collection of pathway maps that represent molecular interactions and reaction networks in cells. Seventy-five of the 126 DEPs identified were annotated, and mapped to a total of six KEGG pathway categories, which included the metabolism, organismal systems, cellular processes, genetic information processing, environmental information processing, and diseases pathway categories (Fig. 4). The annotations in the metabolism, organismal systems, and diseases pathway categories represented 32, 25, and 36 pathway groups, respectively (Fig. 4A, B and F).

The annotations in metabolism pathways category included the carbohydrate, energy, lipid, nucleotide, amino acid, glycan biosynthesis, cofactors and vitamins, biosynthesis of other secondary metabolites, and xenobiotics pathway groups (Fig. 4A). The annotations in the organismal systems category included the Toll-like receptor (TLR) signaling (ko04620), RIG-I-like receptor (RLR) signaling (ko04622), and natural killer cell mediated cytotoxicity (ko04650) pathway groups (Fig. 4B), which represent pathways related primarily to the immune response to virus infection. The largest number of DEPs in the cellular process category were mapped to the lysosome (ko04142) pathway group, all ten of which were down-regulated DEPs (Fig. 4C). The annotations in the genetic information processing category included pathway groups related to DNA replication and repair, transcription, translation, and the folding, sorting, and degradation of proteins (Fig. 4D). The annotations in the environmental information processing

Table 2
The differentially expressed protein lists between PEDV-infected and mock-infected groups.

No.	Protein name	UniProtKB accession no.	GO annotation			*P* value	Average *V*/*C*[b]
			Molecular function	Cellular component	Biological process		
1	Cystatin-C or Cystatin-3	G7PH52	enzyme regulator activity	–	metabolic process; regulation of biological process	6.98E−04	0.46
2[a]	Osteopontin precursor	F7F5L5	–	–	–	9.11E−03	0.50
3	Retinol dehydrogenase 10	G7MZK0	nucleotide binding; catalytic activity	cytoplasm; membrane	development; metabolic process; reproduction; cell differentiation	5.22E−03	0.59
4	Testis cDNA clone	Q4R3Z6	–	–	–	1.36E−03	0.59
5	Overexpressed in colon carcinoma 1 protein	H9FAZ7	–	–	–	6.48E−04	0.61
6	Cytochrome b-245 light chain	H9F3U1	–	membrane	–	1.11E−02	0.62
7[a]	Centrin-2	F7HKU5	metal ion binding; nucleotide binding; catalytic activity	–	–	1.26E−03	0.66
8[a]	Kidney-specific cadherin	F6VCT3	metal ion binding	membrane	–	6.70E−05	0.67
9[a]	Putative WD repeat-containing protein 33	F6SBK9	protein binding	nucleus	–	1.36E−03	0.67
10	Apolipoprotein E4	D5G333	–	extracellular	transport; metabolic process	9.85E−03	0.68
11	Receptor-type tyrosine-protein phosphatase T isoform 1	H9F9X9	catalytic activity	membrane	metabolic process	3.56E−03	0.68
12[a]	Putative neutral and basic amino acid transport protein rBAT-like isoform 3	F7HIT7	catalytic activity	–	metabolic process	8.18E−05	0.69
13[a]	Mitochondrial ornithine aminotransferase	F7BGF3	catalytic activity	cytoplasm; mitochondrion	metabolic process; cell organization and biogenesis	3.51E−02	0.69
14	Lysosomal protective protein	G7N4N3	catalytic activity	nucleus	metabolic process	2.85E-05	0.70
15[a]	Putative low-density lipoprotein receptor-related protein 2	F7H113	metal ion binding; protein binding	cytoplasm; endosome; endoplasmic reticulum; Golgi; membrane	metabolic process; transport; cell proliferation; development	1.02E−04	0.70
16	Alpha-adducin isoform c	H9FPQ1	metal ion binding	cytoskeleton	–	3.58E−03	0.71
17	Integrin beta 2	H9Z8N5	receptor activity; protein binding	membrane	cell communication; regulation of biological process; response to stimulus; development	1.82E−04	0.71
18	Dipeptidyl peptidase 2 preproprotein	H9EXB4	catalytic activity	membrane	metabolic process	4.22E−03	0.71
19[a]	Estrogen sulfotransferase	F6RUQ2	catalytic activity	nucleus; cytoplasm; membrane	metabolic process	4.73E−03	0.71
20[a]	Putative protein EGK_14077	F6PJM4	–	–	–	2.34E−03	0.72
21[a]	Putative legumain	F6S082	catalytic activity	cytoplasm; endosome	response to stimulus; metabolic process; regulation of biological process; cell death	2.53E−03	0.73
22	Metallothionein-1E	F6PYY1	metal ion binding	nucleus; cytoplasm	regulation of biological process; response to stimulus	4.86E−03	0.74
23	Trophoblast glycoprotein	H9F4Q1	protein binding	membrane	–	6.68E−04	0.74
24[a]	Putative proactivator polypeptide isoform X6	F7F376	–	cytoplasm; vacuole	metabolic process	6.40E−03	0.74
25	Cathepsin D (Predicted)	A9L947	catalytic activity	–	metabolic process	1.33E−04	0.75
26	Aldehyde dehydrogenase family 1 member L1	F7HB04	catalytic activity	cytoplasm; mitochondrion	metabolic process	9.07E−03	0.75

Table 2 (*Continued*)

No.	Protein name	UniProtKB accession no.	GO annotation			*P* value	Average *V*/C[b]
			Molecular function	Cellular component	Biological process		
27	Carbonic anhydrase 2	G7MZP3	catalytic activity; metal ion binding	–	metabolic process	1.83E−03	0.75
28	Erythrocyte band 7 integral membrane protein isoform a	F7HP19	–	cytoskeleton; membrane; extracellular	cell organization and biogenesis	4.40E−05	0.75
29[a]	Putative laminin subunit beta-1	F7HPY4	catalytic activity; motor activity; signal transducer activity; protein binding; structural molecule activity; nucleotide binding	extracellular; nucleus; cytoplasm; membrane; cytoskeleton; mitochondrion	metabolic process; regulation of biological process; cell communication; response to stimulus; transport; cellular component movement; development; cell differentiation; cell organization and biogenesis	1.92E−03	0.76
30[a]	Putative tissue alpha-L-fucosidase	F7HDC0	catalytic activity	–	metabolic process	6.56E−03	0.76
31	Similar to human bone marrow stromal cell antigen 1	I7GP78	catalytic activity	–	–	2.77E−02	0.77
32	Solute carrier family 17, member 5	A9X190	–	membrane	transport	8.00E−03	0.77
33	Galectin	G7N3S9	–	–	–	2.88E−03	0.78
34	Sulfhydryl oxidase 2	H9F332	catalytic activity	membrane	metabolic process	4.97E−03	0.78
35	Folate receptor alpha	F7BP60	–	–	–	2.98E−03	0.78
36[a]	Putative protein EGK_10171	G7NLB0	–	–	–	4.60E−03	0.79
37	Lysosome-associated membrane glycoprotein 2 isoform B	F7BCK9	–	membrane	–	1.61E−03	0.79
38	RNA-binding motif protein 12B	G7MZR8	nucleotide binding	membrane	–	2.10E−03	0.79
39	Similar to human synaptobrevin-like 1 (SYBL1)	I7G8H0	–	membrane	transport	8.83E−03	0.79
40[a]	Putative polyadenylate-binding protein-interacting protein 1 isoform 2	F7H0R0	DNA binding; RNA binding; protein binding	–	metabolic process	1.17E−04	0.79
41[a]	Putative versican core protein-like isoform 8	F7C5T5	metal ion binding; protein binding	extracellular	cell differentiation; cellular component movement; development	5.67E−05	0.79
42[a]	Putative N-acetylglucosamine-6-sulfatase	G7PIY5	catalytic activity	cytoplasm; vacuole	metabolic process	1.14E−04	0.80
43	ACADSB	Q5IFK6	catalytic activity; nucleotide binding	–	metabolic process	3.47E−02	0.80
44	Clusterin	Q5ISQ2		–	cell death	2.54E−03	0.80
45	Cathepsin Z	G7N4B3	catalytic activity	–	metabolic process	6.96E−03	0.80
46[a]	Endoplasmic reticulum resident protein 28	F7GNV5	–	cytoplasm; endoplasmic reticulum; organelle lumen	transport	4.49E−02	0.80
47[a]	Putative transducin-like enhancer protein 4 isoform 12	F6PZC8	protein binding	nucleus	metabolic process; regulation of biological process	2.22E−03	0.81
48[a]	T-cell immunoglobulin and mucin domain-containing protein 1	F7GB98	protein binding	–	–	4.71E−05	0.81
49[a]	Putative N-acetylgalactosamine-6-sulfatase	G7NQ90	catalytic activity	–	metabolic process	1.58E−02	0.81
50[a]	Uncharacterized protein	F7GQ07	catalytic activity	–	metabolic process	3.01E−04	0.81
51[a]	Putative galactokinase	F7DF76	nucleotide binding; catalytic activity	cytoplasm	metabolic process	4.72E−02	0.81

Table 2 (*Continued*)

No.	Protein name	UniProtKB accession no.	GO annotation			*P* value	Average *V*/*C*[b]
			Molecular function	Cellular component	Biological process		
52	Signal transducer and activator of transcription	Q9N145	protein binding; DNA binding; signal transducer activity	nucleus; cytoplasm; membrane	cell differentiation; development; metabolic process; regulation of biological process; transport; cell communication; response to stimulus; cell proliferation; reproduction	7.92E−03	0.81
53	Delta(14)-sterol reductase	G7PPJ4	catalytic activity	membrane	metabolic process	3.51E−02	0.81
54[a]	Putative disabled homolog 2 isoform X4	F7GRX9	protein binding	–	–	4.59E−03	0.81
55	Pyridoxal-dependent decarboxylase domain-containing protein 1	F7GW28	catalytic activity	–	metabolic process	1.59E−02	0.81
56	Rho GTPase-activating protein 29	H9FI14	metal ion binding	membrane	cell communication; regulation of biological process; response to stimulus	1.51E−02	0.82
57	Protein DB83	F7H2H1	–	membrane; cytoplasm	–	2.25E−03	0.82
58	DORA reverse strand protein	G7Q0P8	catalytic activity	–	metabolic process	1.01E−02	0.82
59	Bifunctional ATP-dependent dihydroxyacetone kinase/FAD-AMP lyase (Cyclizing)	G7PPY4	catalytic activity; nucleotide binding	membrane	metabolic process	4.96E−03	0.82
60	Cadherin 6	Q5ISM2	metal ion binding	membrane	–	6.61E−03	0.82
61[a]	Putative mitochondrial delta(3,5)-Delta(2,4)-dienoyl-CoA isomerase	F6TNT1	catalytic activity; protein binding	cytoplasm; mitochondrion	metabolic process	5.83E−03	0.82
62	Fatty acid-binding protein, heart	G7MI71	transporter activity	–	transport	2.36E−03	0.82
63[a]	Putative NADH dehydrogenase 1 α subcomplex subunit 8	F7B3T9	–	cytoplasm; mitochon-drion; membrane	–	1.78E−03	0.83
64	Endoplasmic reticulum resident protein 58	G7NJK7	protein binding	cytoplasm; endoplasmic reticulum; organelle lumen	–	5.49E−03	0.83
65	Agrin	H9FU64	transporter activity; protein binding	extracellular; membrane	transport; cell communication; regulation of biological process; response to stimulus; cell organization and biogenesis	9.20E−03	0.83
66[a]	Toll-interacting protein	F7DRQ6	protein binding	–	–	2.53E−02	0.83
67[a]	Putative tetraspanin-3 isoform X2	F6SRI3	–	membrane	–	3.37E−03	0.83
68[a]	Putative protein EGK_14027	G7MM35	enzyme regulator activity; protein binding	cytoplasm; cytoskeleton; membrane	metabolic process; regulation of biological process	6.05E−03	0.83
69	Inosine-5′-monophosphate dehydrogenase	F6VXT4	nucleotide binding; catalytic activity; protein binding; metal ion binding	nucleus; cytoplasm; membrane	metabolic process; cell proliferation; response to stimulus	3.12E−04	1.20
70	78 kDa glucose-regulated protein	F7C3R1	nucleotide binding; catalytic activity; protein binding	nucleus; cytoplasm; endoplasmic reticulum; cell surface; membrane	cell organization and biogenesis; cell communication; regulation of biological process; response to stimulus; metabolic process; development; cell death	9.49E−05	1.20
71[a]	Uncharacterized protein	F6W6U2	–	–	–	1.40E−02	1.20

Table 2 (*Continued*)

No.	Protein name	UniProtKB accession no.	GO annotation			*P* value	Average *V*/C[b]
			Molecular function	Cellular component	Biological process		
72[a]	Follistatin-related protein 1	G7MKF2	metal ion binding; protein binding	–	–	3.29E−04	1.20
73[a]	Putative retrotransposon-like protein 1	F7G2J3	RNA binding; catalytic activity	–	metabolic process	6.78E−04	1.20
74[a]	Heat shock protein 105 kDa	F6S529	nucleotide binding	–	–	6.60E−05	1.21
75[a]	Putative protein midA homolog	F7GTQ7	–	–	–	2.96E−03	1.21
76	Similar to human S-adenosylhomocysteine hydrolase-like 1	I7GBN2	catalytic activity	–	metabolic process; transport	9.34E−03	1.21
77	Transferrin receptor 1	F6UX47	catalytic activity	extracellular; cytoplasm; endosome; membrane; cell surface	metabolic process; cellular homeostasis; cell differentiation; development; regulation of biological process	4.64E−04	1.22
78[a]	Exocyst complex component 6B	F7GZR4	–	cytoplasm	transport	5.75E−03	1.22
79	Protein S100-A2	H9F670	metal ion binding	membrane	–	4.75E−02	1.22
80[a]	Ephrin type-A receptor 2	F7E018	nucleotide binding; catalytic activity; receptor activity; signal transducer activity; protein binding	membrane	development; cell differentiation; metabolic process; cell communication; regulation of biological process; response to stimulus; cell death; cell organization and biogenesis; cell proliferation; cellular component movement	3.02E−02	1.22
81[a]	Putative nucleolar RNA helicase 2-like isoform 3	F6SQP8	nucleotide binding; RNA binding; catalytic activity	nucleus	–	1.12E−03	1.23
82[a]	Putative polyadenylate-binding protein 1-like isoform X2	F7EU27	nucleotide binding; RNA binding	–	–	1.77E−03	1.23
83[a]	Uncharacterized protein	F7CEU8	nucleotide binding	–	–	5.52E−03	1.23
84	Sequestosome-1 isoform 1	I2CY26	metal ion binding	–	–	8.51E−03	1.23
85	NEDD8 ultimate buster 1 isoform 2	H9EZG1	protein binding	–	metabolic process; regulation of biological process; defense response; response to stimulus	2.32E−02	1.23
86	Thioredoxin domain-containing protein 9	F6YEB0	–	nucleus; cytoplasm; cytoskeleton	cellular homeostasis; regulation of biological process	3.79E−02	1.23
87	Four and a half LIM domains protein 2	F7GXH4	protein binding; metal ion binding	nucleus; cytoskeleton	metabolic process; regulation of biological process; cell differentiation; response to stimulus; cell death; development	2.24E−05	1.23
88	Similar to human DKFZP564M182 protein	I7G2J1	RNA binding; structural molecule activity	cytoplasm; ribosome	metabolic process	2.95E−03	1.23
89	Similar to human hypothetical protein FLJ10634	I7GMW8	nucleotide binding	–	–	1.69E−02	1.23
90[a]	Putative hexokinase-2	F6Y855	nucleotide binding; catalytic activity	cytoplasm; membrane; mitochondrion	metabolic process	3.26E−04	1.24
91	Ribosomal protein L37	F7FYI2	RNA binding; structural molecule activity; metal ion binding	cytoplasm; ribosome; cytosol	metabolic process	3.51E−03	1.24
92	Pyruvate kinase	F7FI39	metal ion binding; catalytic activity	–	metabolic process	1.07E−02	1.24

Table 2 (*Continued*)

No.	Protein name	UniProtKB accession no.	GO annotation			*P* value	Average *V*/*C*[b]
			Molecular function	Cellular component	Biological process		
93	Protein phosphatase 1B isoform 2	H9EM08	metal ion binding; catalytic activity	–	metabolic process	1.40E−02	1.24
94[a]	Glycogen synthase kinase-3 alpha	G7PXQ8	nucleotide binding; catalytic activity	membrane	metabolic process	4.34E−03	1.24
95	Phosphoserine aminotransferase	F7H2J8	catalytic activity	–	metabolic process	1.01E−03	1.25
96	Histone H2A	H9FCA2	DNA binding; protein binding	chromosome; nucleus; membrane	cell organization and biogenesis; metabolic process	2.02E−03	1.25
97	EF-hand domain-containing protein D2	H9FC53	metal ion binding	–	–	6.88E−04	1.25
98[a]	Putative ATP-dependent RNA helicase DDX10	F7BIN5	nucleotide binding; catalytic activity	–	–	1.20E−04	1.25
99[a]	Putative pterin-4-alpha-carbinolamine dehydratase	F7F694	catalytic activity; protein binding	nucleus; cytoplasm	metabolic process; cell organization and biogenesis	1.85E−02	1.26
100	Integrin beta 3	F7FG54	receptor activity; protein binding	membrane; cell surface	cell organization and biogenesis; cell communication; regulation of biological process; response to stimulus; development; cellular component movement; cell proliferation; coagulation	2.60E−04	1.26
101	Similar to human exocyst complex component 7	I7GLB8	–	cytoplasm	transport	5.30E−03	1.27
102[a]	Putative leucine-rich repeat flightless-interacting protein 1	F6S3D2	–	–	–	1.48E−03	1.27
103[a]	Uncharacterized protein	G7P460	–	–	–	8.80E−04	1.28
104	Eukaryotic initiation factor 4A-I isoform 1	H9FAB5	nucleotide binding; RNA binding; catalytic activity	cytoplasm	metabolic process	2.51E−03	1.29
105[a]	Phosphatidylinositol transfer protein beta isoform isoform 2	F7G7C8	–	–	transport	1.70E−02	1.29
106	Phosphatidylinositol-3,4,5-trisphosphate 5-phosphatase 2	G7NE91	protein binding	–	metabolic process	4.14E−03	1.30
107[a]	Putative tripartite motif-containing protein 47 (TRIM47)	F7HF49	protein binding; metal ion binding	intracellular	–	2.65E−02	1.31
108	UDP-N-acetylhexosamine pyrophosphorylase	F7CXU2	catalytic activity	–	metabolic process	3.83E−02	1.32
109[a]	Putative protein EGK_20713	F7B9G5	protein binding	–	–	3.42E−03	1.32
110[a]	Putative 60S ribosomal protein L23a-like	F7HD49	nucleotide binding; structural molecule activity	cytoplasm; ribosome	metabolic process	3.89E−04	1.33
111	Mitochondrial import inner membrane translocase subunit Tim13	F6R7Z6	metal ion binding	cytoplasm; mitochondrion	cell organization and biogenesis; transport	1.98E−04	1.33
112	Poly [ADP-ribose] polymerase 9 isoform c	H9ZE68	catalytic activity	membrane	–	3.46E−03	1.34
113[a]	Serpin B6	F7BRQ5	enzyme regulator activity	extracellular	–	7.69E−04	1.35
114	EH domain-containing protein 4	F7HAE5	catalytic activity; metal ion binding; protein binding; nucleotide binding	cytoplasm; endoplasmic reticulum; endosome; membrane	metabolic process; transport; cell organization and biogenesis	2.73E−04	1.35
115	Calponin-like integrin-linked kinase-binding protein	G7PQP7	protein binding; catalytic activity	membrane	cell communication; regulation of biological process; response to stimulus; metabolic process	5.57E−04	1.35

Table 2 (*Continued*)

No.	Protein name	UniProtKB accession no.	GO annotation			*P* value	Average *V*/*C*[b]
			Molecular function	Cellular component	Biological process		
116[a]	Putative protein EGK_00649	G8F2R2	transporter activity	membrane	transport	2.83E−03	1.36
117	Ribosomal RNA-processing protein 8	F7C3H4	catalytic activity; protein binding	nucleus; organelle lumen; cytoplasm; membrane; chromosome	metabolic process; regulation of biological process; cell communication; response to stimulus; cell death	3.59E−03	1.36
118	Microtubule-associated protein 1B	G7P7P5	protein binding; catalytic activity	cytoskeleton; membrane	cell organization and biogenesis	3.37E−05	1.37
119	FMRP-interacting protein 2	G7NGR9	–	–	–	3.95E−04	1.42
120[a]	Putative centrosomal protein of 89 kDa isoform X1	F7H5V4	protein binding	–	–	8.26E−04	1.44
121[a]	Ubiquitin-conjugating enzyme	F6ULI1	catalytic activity	–	–	3.58E−03	1.49
122	Nucleolar complex protein 14	G7NVR8	–	membrane	–	4.14E−07	1.52
123	Ubiquitin-like protein ISG15	F7GS84	protein binding	extracellular	metabolic process; regulation of biological process; defense response; response to stimulus	1.59E−05	1.76
124[a]	Putative caspase-7 isoform X1	G7PDZ9	catalytic activity	cytoplasm	metabolic process; cell death	2.21E−04	1.76
125[a]	Putative tRNA pseudouridine synthase Pus10	H9FK14	–	–	–	2.56E−04	2.21
126	OCIA domain-containing protein 1 isoform 2	H9FWA7	–	membrane	–	1.20E−02	2.50

[a] The names of the uncharacterized/putative proteins were annotated again and corrected by the blastp search in GenBank database of NCBI based on the primary identified protein sequences from the UniProtKB.

[b] The average *V*/*C* ratio >1 represents the up-regulated proteins; the average *V*/*C* ratio <1 represents the down-regulated proteins.

category included the PI3K-Akt signaling (ko04151), mitogen-activated protein kinase (MAPK) signaling (ko04010), Jak-STAT signaling (ko04630), TNF signaling (ko04668), and cell adhesion molecule (ko04514) pathway groups (Fig. 4E), all of which represented signal transduction and signaling-molecule interactions that have been shown to be associated with virus infection. The annotations in the diseases category included the human T-cell leukemia virus infection, Epstein–Barr virus infection, hepatitis C, hepatitis B, and measles pathway groups (Fig. 4F), all of which are associated with virus infection involving in three down-regulated

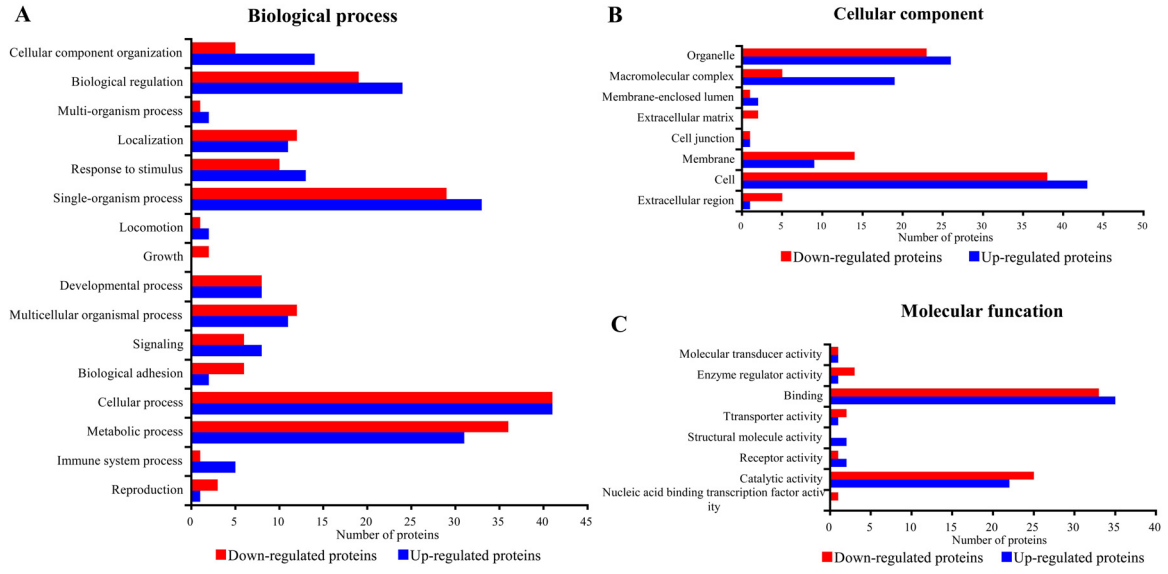

Fig. 3. The Gene Ontology (GO) categories of the differentially expressed proteins at level 2. (A) Biological process GO categories; (B) cellular component GO categories; (C) molecular function GO categories.

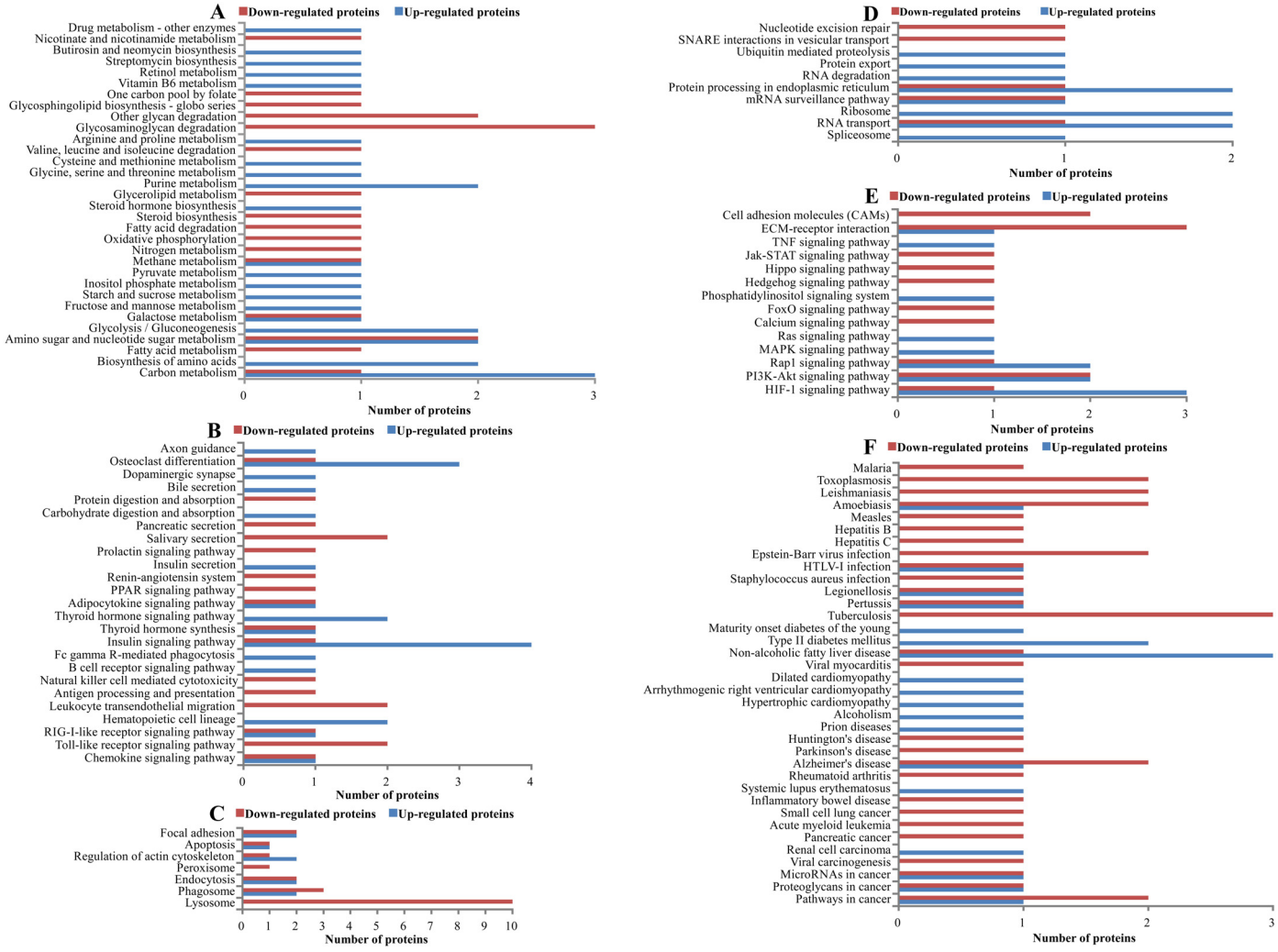

Fig. 4. Analysis of the KEGG pathway of the differentially expressed proteins. (A) Metabolism; (B) organismal systems; (C) cellular processes; (D) genetic information processing; (E) environmental information processing; (F) diseases.

proteins and one up-regulated protein. Overall, more disease pathway groups were assigned to a single down-regulated DEP than those assigned to up-regulated DEPs. The integrin (β2 and β3 subunits) protein was annotated to the largest number of pathway groups (28), which included the organismal systems, environmental information processing, cellular processes, and diseases categories.

3.4. *Verification of differential expression*

The β tubulin as loading control, three down-regulated DEPs cystatin-C, apolipoprotein E4 and centrin-2, two up-regulated DEPs integrin-β3 and protein S100-A2, were selected to verify differential expression between the PEDV-infected and mock-infected Vero E6 cells. The immunoblotting analysis showed that the ratios of these proteins between the PEDV-infected and mock-infected groups were consistent with those obtained using the quantitative proteomics analysis (Fig. 5).

4. Discussion

In our study, PEDV infection significantly alters protein expression in Vero E6 cells. The differentially expressed proteins (DEPs) annotated to virus infection-associated signaling pathways, autophagy, and virus entry-associated proteins were analyzed further to assess their potential roles in PEDV infection. In mammals, the first line of defense against virus infection is the innate immune system. Early antiviral responses are initiated upon the recognition of pathogen-associated molecular patterns (PAMPs) by pattern recognition receptors (PRRs), resulting in the production of interferons for the innate immune response and the maturation of dendritic cells for establishing acquired immunity (Yokota et al., 2010). The PRRs are grouped into the TLRs, RLRs, and nucleotide binding-oligomerization domain-like receptors. Our results showed that PEDV infection induced the DEPs that participated in six signaling pathways involved in viral infection, including the RLR, Rap1, PI3K-Akt, MAPK, Jak-STAT, and TLR signaling pathways.

The PEDV is an enteric virus that infects the intestinal epithelial cells (IEC) of swine, causing severe diarrhea. Hirata et al. (2007) reported the RIG-I signaling pathway plays an important role in antiviral innate immunity mechanisms in IECs. Sheikh et al. (2013) reported the Rap1A signaling pathway was associated with secretory diarrhea. The Jak-STAT signaling pathway regulates the adaptive and innate mechanisms related to mucosal immunity (Heneghan et al., 2013; Wang et al., 2013). Our results showed that DEPs induced by PEDV infection in Vero E6 cells involved in the RLR, Rap1, and Jak-STAT signaling pathways. It has been reported that the TLR, MAPK, and PI3K-Akt signaling pathways play roles in host cell responses to coronaviruses (Mizutani et al., 2004; Mizutani

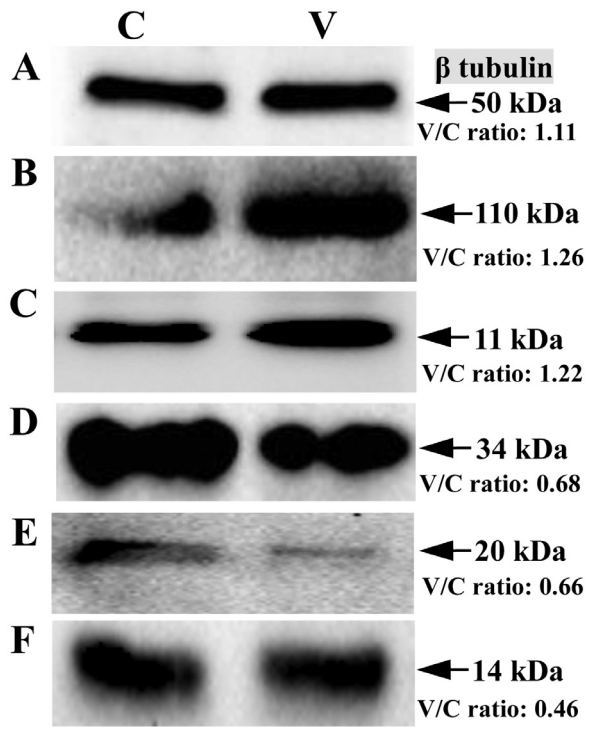

Fig. 5. Verification of the selected differential expression proteins by western blot. (A) β tubulin; (B) Integrin β3; (C) Protein S100-A2; (D) Apolipoprotein E4; (E) Centrin-2; (F) Cystatin-C. The iTRAQ quantitative ratio "*V*/*C* ratio" is shown in Figure.

et al., 2005; Mazaleuskaya et al., 2012). Our results demonstrate that the recognition of viral PAMPs by PRRs may mediate antiviral signaling in PEDV-infected Vero E6 cells.

Integrins are cell surface α/β heterodimeric glycoproteins that contribute to a variety of cellular functions (Stewart and Nemerow, 2007). Combinations of the various isotypes of the α and β subunits of integrins generate more than 20 different integrin proteins. Previous studies have shown that various integrin molecules are used as receptors for virus attachment (Stewart and Nemerow, 2007; Sun et al., 2013). In our current study, the expression of integrin-β2 and -β3 was down-regulated and up-regulated, respectively, in response to PEDV infection. The upregulation of integrin-β3 expression is consistent with that observed in response to dengue virus infection (Zhang et al., 2007). Our pathway analysis revealed that both integrin-β2 and -β3 are involved in 28 pathways that contribute to organismal systems, environmental information processing, cellular processes, and diseases.

The integrin αvβ3 protein has been shown to serve as an entry receptor for various viruses (Guerrero et al., 2000; Neff et al., 2000; Chu and Ng, 2004; Parry et al., 2005; Wang et al., 2005), some of which bind the integrin through an RGD sequence in a viral structural protein to initiate infection (Stewart and Nemerow, 2007). The S protein of PEDV is a glycoprotein peplomer on the viral surface that plays an important role in receptor-mediated binding and cell membrane fusion. In our study, the integrin recognized sequences of PEDV S protein was analyzed based on Ruoslahti's (1996) report. The results indicated that four conserved integrin-recognized amino acid motifs (Asp-Gly-Glu, Lys-Gly-Glu, Arg-Leu-Asp, and Leu-Asp-Val) were found in the S proteins of various PEDV strains (data not shown). These data suggest that integrin proteins may act as an infection associated protein for the attachment and entry of PEDV.

Autophagy is an essential component of host defenses against viral infection (Dong and Levine, 2013). Maier and Britton (2012) reported that β-coronaviruses induced autophagy. In our study, more DEPs were mapped to the autophagy pathway group than any of the other pathway groups. Fifteen DEPs were mapped to the lysosome and phagosome pathways. Of the 15 proteins, 12 (80%) were down-regulated DEPs. Although the autophagy pathway plays an antiviral role in virus-infected cells, the autophagy machinery is exploited by certain viruses for viral evasion and propagation. Our results showed that PEDV infection induced the downregulation of the expression of many autophagy-associated proteins. Therefore, PEDV infection might inhibit autophagy in Vero E6 cells, thus facilitating virus replication. Previous studies have shown that the microtubule-associated protein 1B is a useful biomarker protein for autophagy (Dong and Levine, 2013). We found that the expression of MAP1B was up-regulated 1.37-fold in the PEDV-infected Vero E6 cells. These results suggest that the PEDV induces autophagy.

Cystatin-C has been shown to reduce the replication of certain viruses, including the poliovirus, rhinovirus, and human coronaviruses OC43 and 229E (Korant et al., 1986; Collins and Grubb, 1991). The cleavage of S protein has been shown to be essential for the induction of cell-to-cell fusion and coronavirus entry into cells (Sturman et al., 1985). Shirato et al. (2011) reported the transmembrane type II serine protease 2 enhanced infection of PEDV in Vero cells by increasing virus release. In our study, the reduced expression of cystatin-C might facilitate PEDV replication and release through the activation of cysteine-associated proteases in Vero E6 cells. Apolipoprotein E4, galectin, clusterin, and transferrin receptor 1 have also been shown to be associated with virus infection (Hishiki et al., 2010; Peng et al., 2011; Martin and Uprichard, 2013; Tripathi et al., 2013), and may therefore function as infection-associated proteins in PEDV-infected Vero E6 cells. Additionally, the decreased in vitro expression of the adherens junction protein, such as cadherin, might be associated with a reduced integrity of PEDV-infected intestinal epithelial cells in vivo.

To the best of our knowledge, our study represents the analysis of the interactions between PEDV and Vero E6 cells using a quantitative proteomics technique. PEDV infection-associated pathways and proteins are described and discussed based on the bioinformatics analysis of the differentially expressed proteins. Our analysis of Vero E6 cell responses to PEDV infection identified relevant targets for subsequent in-depth studies of PEDV pathogenesis, expand the current knowledge base regarding the interaction between the PEDV and the host cell, and provide useful basic information about other coronaviruses. Although the Vero E6 cells are highly susceptible to PEDV infection and facilitate experimental design and performance for proteomics, the Vero E6 cell line is an interferon-deficient cell line and not a pig cell line. So, the detailed functions of these pathways and proteins in PEDV infection require further verification in the actual host cells of PEDV.

Acknowledgments

This work is supported by the National Natural Science Foundation of China (grant no. 31472209), the State National Key Laboratory of Veterinary Biotechnology (grant no. SKLVBF201506/201302), and the Program for New Century Excellent Talents in Heilongjiang Provincial University (grant no. 1252-NCET-016).

References

Ashburner, M., Ball, C.A., Blake, J.A., Botstein, D., Butler, H., Cherry, J.M., Davis, A.P., Dolinski, K., Dwight, S.S., Eppig, J.T., Harris, M.A., Hill, D.P., Issel-Tarver, L., Kasarskis, A., Lewis, S., Matese, J.C., Richardson, J.E., Ringwald, M., Rubin, G.M., Sherlock, G., 2000. Gene ontology: tool for the unification of biology. The Gene Ontology Consortium. Nat. Genet. 25, 25–29.

Belouzard, S., Millet, J.K., Licitra, B.N., Whittaker, G.R., 2012. Mechanisms of coronavirus cell entry mediated by the viral spike protein. Viruses 4, 1011–1033.

Boja, E., Hiltke, T., Rivers, R., Kinsinger, C., Rahba, A., Mesri, M., Rodriguez, H., 2011. Evolution of clinical proteomics and its role in medicine. J. Proteome Res. 10, 66–84.
Chen, J., Liu, X., Shi, D., Shi, H., Zhang, X., Li, C., Chi, Y., Feng, L., 2013. Detection and molecular diversity of spike gene of porcine epidemic diarrhea virus in China. Viruses 5, 2601–2613.
Chen, J., Wang, C., Shi, H., Qiu, H., Liu, S., Chen, X., Zhang, Z., Feng, L., 2010. Molecular epidemiology of porcine epidemic diarrhea virus in China. Arch. Virol. 155, 1471–1476.
Chen, Q., Li, G., Stasko, J., Thomas, J.T., Stensland, W.R., Pillatzki, A.E., Gauger, P.C., Schwartz, K.J., Madson, D., Yoon, K.J., Stevenson, G.W., Burrough, E.R., Harmon, K.M., Main, R.G., Zhang, J., 2014. Isolation and characterization of porcine epidemic diarrhea viruses associated with the 2013 disease outbreak in US swine. J. Clin. Microbiol. 52, 234–243.
Chu, J.J., Ng, M.L., 2004. Interaction of West Nile virus with alpha v beta 3 integrin mediates virus entry into cells. J. Biol. Chem. 279, 54533–54541.
Collins, A.R., Grubb, A., 1991. Inhibitory effects of recombinant human cystatin C on human coronaviruses. Antimicrob. Agents Chemother. 35, 2444–2446.
Dong, X., Levine, B., 2013. Autophagy and viruses: adversaries or allies? J. Innate Immun. 5, 480–493.
Götz, S., García-Gómez, J.M., Terol, J., Williams, T.D., Nagaraj, S.H., Nueda, M.J., Robles, M., Talón, M., Dopazo, J., Conesa, A., 2008. High-throughput functional annotation and data mining with the Blast2GO suite. Nucleic Acids Res. 36, 3420–3435.
Guerrero, C.A., Méndez, E., Zárate, S., Isa, P., López, S., Arias, C.F., 2000. Integrin alpha(v)beta(3) mediates rotavirus cell entry. Proc. Natl. Acad. Sci. U.S.A. 97, 14644–14649.
Guo, D., Zhu, Q., Feng, L., Sun, D., 2013. Screening and antiviral analysis of phages that display peptides with an affinity to subunit C of porcine aminopeptidase. Monoclon. Antib. Immunodiagn. Immunother. 32, 326–329.
Guo, D., Zhu, Q., Zhang, H., Sun, D., 2014. Proteomic analysis of membrane proteins of vero cells: Exploration of potential proteins responsible for virus entry. DNA Cell Biol. 33, 20–28.
He, Y., Li, W., Liao, G., Xie, J., 2012. Mycobacterium tuberculosis-specific phagosome proteome and underlying signaling pathways. J. Proteome Res. 11, 2635–2643.
Heneghan, A.F., Pierre, J.F., Kudsk, K.A., 2013. JAK-STAT and intestinal mucosal immunology. JAKSTAT 2, e25530.
Hirata, Y., Broquet, A.H., Menchén, L., Kagnof, M.F., 2007. Activation of innate immune defense mechanisms by signaling through RIG-I/IPS-1 in intestinal epithelial cells. J. Immunol. 179, 5425–5432.
Hishiki, T., Shimizu, Y., Tobita, R., Sugiyama, K., Ogawa, K., Funami, K., Ohsaki, Y., Fujimoto, T., Takaku, H., Wakita, T., Baumert, T.F., Miyanari, Y., Shimotohno, K., 2010. Infectivity of hepatitis C virus is influenced by association with apolipoprotein E isoforms. J. Virol. 84, 12048–12057.
Hofmann, M., Wyler, R., 1988. Propagation of the virus of porcine epidemic diarrhea in cell culture. J. Clin. Microbiol. 26, 2235–2239.
Hondermarck, H., Tastet, C., El Yazidi-Belkoura, I., Toillon, R.A., Le Bourhis, X., 2008. Proteomics of breast cancer: the quest for markers and therapeutic targets. J. Proteome Res. 7, 1403–1411.
Huang, Y.W., Dickerman, A.W., Piñeyro, P., Li, L., Fang, L., Kiehne, R., Opriessnig, T., Meng, X.J., 2013. Origin, evolution, and genotyping of emergent porcine epidemic diarrhea virus strains in the United States. MBio 4, e00737–e813.
Kanehisa, M., Goto, S., Sato, Y., Furumichi, M., Tanabe, M., 2012. KEGG for integration and interpretation of large-scale molecular data sets. Nucleic Acids Res. 40, 109–114.
Kim, Y., Lee, C., 2013. Ribavirin efficiently suppresses porcine nidovirus replication. Virus Res. 171, 44–53.
Korant, B.D., Towatari, T., Ivanoff, L., Petteway, S.J., Brzin, J., Lenarcic, B., Turk, V., 1986. Viral therapy: prospects for protease inhibitors. J. Cell Biochem. 32, 91–95.
Li, W., Li, H., Liu, Y., Pan, Y., Deng, F., Song, Y., Tang, X., He, Q., 2012. New variants of porcine epidemic diarrhea virus, China, 2011. Emerg. Infect. Dis. 18, 1350–1353.
Linde, M.E., Colquhoun, D.R., Mohien, C.U., Kole, T., Aquino, V., Cotter, R., Edwards, N., Hildreth, J.E., Graham, D.R., 2013. The conserved set of host proteins incorporated into HIV-1 virions suggests a common egress pathway in multiple cell types. J. Proteome Res. 12, 2045–2054.
Maier, H.J., Britton, P., 2012. Involvement of autophagy in coronavirus replication. Viruses 4, 3440–3451.
Marthaler, D., Jiang, Y., Otterson, T., Goyal, S., Rossow, K., Collins, J., 2013. Complete genome sequence of porcine epidemic diarrhea virus strain USA/Colorado/2013 from the United States. Genome Announc. 1, e00555–e613.
Martin, D.N., Uprichard, S.L., 2013. Identification of transferrin receptor 1 as a hepatitis C virus entry factor. Proc. Natl. Acad. Sci. U.S.A. 110, 10777–10782.
Mazaleuskaya, L., Veltrop, R., Ikpeze, N., Martin-Garcia, J., Navas-Martin, S., 2012. Protective role of Toll-like Receptor 3-induced type I interferon in murine coronavirus infection of macrophages. Viruses 4, 901–923.
Mizutani, T., Fukushi, S., Murakami, M., Hirano, T., Saijo, M., Kurane, I., Morikawa, S., 2004. Tyrosine dephosphorylation of STAT3 in SARS coronavirus-infected Vero E6 cells. FEBS Lett. 577, 187–192.
Mizutani, T., Fukushi, S., Saijo, M., Kurane, I., Morikawa, S., 2005. JNK and PI3k/Akt signaling pathways are required for establishing persistent SARS-CoV infection in Vero E6 cells. Biochim. Biophys. Acta 1741, 4–10.
Neff, S., Mason, P.W., Baxt, B., 2000. High-efficiency utilization of the bovine integrin alpha(v)beta(3) as a receptor for foot-and-mouth disease virus is dependent on the bovine beta(3) subunit. J. Virol. 74, 7298–7306.
Pan, Y., Tian, X., Li, W., Zhou, Q., Wang, D., Bi, Y., Chen, F., Song, Y., 2012. Isolation and characterization of a variant porcine epidemic diarrhea virus in China. Virol. J. 9, 195.
Papachristou, E.K., Roumeliotis, T.I., Chrysagi, A., Trigoni, C., Charvalos, E., Townsend, P.A., Pavlakis, K., Garbis, S.D., 2013. The shotgun proteomic study of the human ThinPrep cervical smear using iTRAQ mass-tagging and 2D LC-FT-Orbitrap-MS: the detection of the human papillomavirus at the protein level. J. Proteome Res. 12, 2078–2089.
Parry, C., Bell, S., Minson, T., Browne, H., 2005. Herpes simplex virus type 1 glycoprotein H binds to alphavbeta3 integrins. J. Gen. Virol. 86, 7–10.
Peng, G., Sun, D., Rajashankar, K.R., Qian, Z., Holmes, K.V., Li, F., 2011. Crystal structure of mouse coronavirus receptor-binding domain complexed with its murine receptor. Proc. Natl. Acad. Sci. U.S.A. 108, 10696–10701.
Pensaert, M.B., Debouck, P., 1978. A new coronavirus-like particle associated with diarrhea in swine. Arch. Virol. 58, 243–247.
Puranaveja, S., Poolperm, P., Lertwatcharasarakul, P., Kesdaengsakonwut, S., Boonsoongnern, A., Urairong, K., Kitikoon, P., Choojai, P., Kedkovid, R., Teankum, K., Thanawongnuwech, R., 2009. Chinese-like strain of porcine epidemic diarrhea virus, Thailand. Emerg. Infect. Dis. 15, 1112–1115.
Quevillon, E., Silventoinen, V., Pillai, S., Harte, N., Mulder, N., Apweiler, R., Lopez, R., 2005. InterProScan: protein domains identifier. Nucleic Acids Res. 33, 116–120.
Ren, X., Suo, S., Jang, Y.S., 2011. Development of a porcine epidemic diarrhea virus M protein-based ELISA for virus detection. Biotechnol. Lett. 33, 215–220.
Ruoslahti, E., 1996. RGD and other recognition sequences for integrins. Annu. Rev. Cell Dev. Biol. 12, 697–715.
Sheikh, I.A., Koley, H., Chakrabarti, M.K., Hoque, K.M., 2013. The Epac1 signaling pathway regulates Cl^- secretion via modulation of apical KCNN4c channels in diarrhea. J. Biol. Chem. 288, 20404–20415.
Shirato, K., Matsuyama, S., Ujike, M., Taguchi, F., 2011. Role of proteases in the release of porcine epidemic diarrhea virus from infected cells. J. Virol. 85, 7872–7880.
Stevenson, G.W., Hoang, H., Schwartz, K.J., Burrough, E.R., Sun, D., Madson, D., Cooper, V.L., Pillatzki, A., Gauger, P., Schmitt, B.J., Koster, L.G., Killian, M.L., Yoon, K.J., 2013. Emergence of porcine epidemic diarrhea virus in the United States: clinical signs, lesions, and viral genomic sequences. J. Vet. Diagn. Invest. 25, 649–654.
Stewart, P.L., Nemerow, G.R., 2007. Cell integrins: commonly used receptors for diverse viral pathogens. Trends Microbiol. 15, 500–507.
Sturman, L.S., Ricard, C.S., Holmes, K.V., 1985. Proteolytic cleavage of the E2 glycoprotein of murine coronavirus: activation of cell-fusing activity of virions by trypsin and separation of two different 90 K cleavage fragments. J. Virol. 56, 904–911.
Sun, D., Shi, H., Chen, J., Shi, D., Zhu, Q., Zhang, H., Liu, S., Wang, Y., Qiu, H., Feng, L., 2012. Generation of a mouse scFv library specific for porcine aminopeptidase N using the T7 phage display system. J. Virol. Methods 182, 99–103.
Sun, D., Zhang, H., Guo, D., Sun, A., Wang, H., 2013. Shotgun proteomic analysis of plasma from dairy cattle suffering from footrot: characterization of potential disease-associated factors. PLoS ONE 8, e55973.
Sun, D.B., Feng, L., Shi, H.Y., Chen, J.F., Cui, X.C., Chen, H.Y., Liu, S.W., Tong, Y.E., Wang, Y.F., Tong, G.Z., 2008. Identification of two novel B cell epitopes on porcine epidemic diarrhea virus spike protein. Vet. Microbiol. 131, 73–81.
Tripathi, S., Batra, J., Cao, W., Sharma, K., Patel, J.R., Ranjan, P., Kumar, A., Katz, J.M., Cox, N.J., Lal, R.B., Sambhara, S., Lal, S.K., 2013. Influenza A virus nucleoprotein induces apoptosis in human airway epithelial cells: implications of a novel interaction between nucleoprotein and host protein Clusterin. Cell Death Dis. 4, e562.
Unwin, R.D., Griffiths, G.R., Whetton, A.D., 2010. Simultaneous analysis of relative protein expression levels across multiple samples using iTRAQ isobaric tags with 2D nano LC–MS/MS. Nat. Protoc. 5, 1574–1582.
Wang, R., Nan, Y., Yu, Y., Zhang, Y.J., 2013. Porcine reproductive and respiratory syndrome virus Nsp1β inhibits interferon-activated JAK/STAT signal transduction by inducing karyopherin-α1 degradation. J. Virol. 87, 5219–5228.
Wang, X., Huang, D.Y., Huong, S.M., Huang, E.S., 2005. Integrin alphavbeta3 is a coreceptor for human cytomegalovirus. Nat. Med. 11, 515–521.
Wiśniewski, J.R., Zougman, A., Nagaraj, N., Mann, M., 2009. Universal sample preparation method for proteome analysis. Nat. Methods 6, 359–362.
Yang, X., Huo, J.Y., Chen, L., Zheng, F.M., Chang, H.T., Zhao, J., Wang, X.W., Wang, C.Q., 2013. Genetic variation analysis of reemerging porcine epidemic diarrhea virus prevailing in central China from 2010 to 2011. Virus Genes 46, 337–344.
Ye, Y., Yan, G., Luo, Y., Tong, T., Liu, X., Xin, C., Liao, M., Fan, H., 2013. Quantitative proteomics by amino acid labeling in foot-and-mouth disease virus (FMDV)-infected cells. J. Proteome Res. 12, 363–377.
Yokota, S., Okabayashi, T., Fujii, N., 2010. The battle between virus and host: modulation of Toll-like receptor signaling pathways by virus infection. Mediators Inflamm. 2010, 184328.
Yuan, J., Gao, H., Sui, J., Duan, H., Chen, W.N., Ching, C.B., 2012. Cytotoxicity evaluation of oxidized single-walled carbon nanotubes and graphene oxide on human hepatoma HepG2 cells: an iTRAQ-coupled 2D LC–MS/MS proteome analysis. Toxicol. Sci. 126, 149–161.
Zeng, S., Zhang, H., Ding, Z., Luo, R., An, K., Liu, L., Bi, J., Chen, H., Xiao, S., Fang, L., 2015. Proteome analysis of porcine epidemic diarrhea virus (PEDV)-infected vero cells. Proteomics 2015 Jan 20, http://dx.doi.org/10.1002/pmic.201400458, PubMed PMID: 25604190 (epub ahead of print).
Zhang, J.L., Wang, J.L., Gao, N., Chen, Z.T., Tian, Y.P., An, J., 2007. Up-regulated expression of beta3 integrin induced by dengue virus serotype 2 infection associated with virus entry into human dermal microvascular endothelial cells. Biochem. Biophys. Res. Commun. 356, 763–768.
Zhu, Q., Guo, D., Feng, L., Sun, D., 2013. Expression and purification of the scFv from hybridoma cells secreting a monoclonal antibody against S Protein of PEDV. Monoclon. Antib. Immunodiagn. Immunother. 32, 41–46.